Published as: *Curr Biol*. 2008 April 8; 18(7): 481–489.

Distinct innate immune responses to infection and wounding in the *C. elegans* epidermis

Nathalie Pujol[1,2,3,7], **Sophie Cypowyj**[1,2,3,7], **Katja Ziegler**[1,2,3], **Anne Millet**[1,2,3], **Aline Astrain**[1,2,3], **Alexandr Goncharov**[4,5], **Yishi Jin**[4,5], **Andrew D. Chisholm**[4], and **Jonathan J. Ewbank**[1,2,3,6]

1 *Centre d'Immunologie de Marseille-Luminy, Université de la Méditerranée, Case 906, 13288 Marseille cedex 9, France*

2 *INSERM, U631, 13288 Marseille, France*

3 *CNRS, UMR6102, 13288 Marseille, France*

4 *Division of Biological Sciences, University of California San Diego, 9500 Gilman Drive, La Jolla, CA 92093, USA*

5 *Howard Hughes Medical Institute*

Summary

Background—In many animals, the epidermis is in permanent contact with the environment and represents a first line of defense against pathogens and injury. Infection of the nematode *Caenorhabditis elegans* by the natural fungal pathogen *Drechmeria coniospora* induces the expression in the epidermis of antimicrobial peptide (AMP) genes such as *nlp-29*. Here, we tested the hypothesis that injury might also alter AMP gene expression and sought to characterize the mechanisms that regulate the innate immune response.

Results—Injury induces a wound-healing response in *C. elegans* that includes induction of *nlp-29* in the epidermis. We find that a conserved p38-MAP kinase cascade is required in the epidermis for the response to both infection and wounding. Through a forward genetic screen, we isolated mutants that failed to induce *nlp-29* expression after *D. coniospora* infection. We identify a kinase, NIPI-3, related to human Tribbles homolog 1, that is likely to act upstream of the MAP2K SEK-1. We find NIPI-3 is required only for *nlp-29* induction following infection and not following wounding.

Conclusions—Our results show that the *C. elegans* epidermis actively responds to wounding and infection via distinct pathways that converge on a conserved signaling cassette that controls the expression of the AMP gene *nlp-29*. A comparison between these results and MAP kinase signaling in yeast gives insights into the possible origin and evolution of innate immunity.

Introduction

The nematode *C. elegans* responds to bacterial infection by up-regulating the expression of genes encoding antimicrobial proteins [1–5]. Although it is not known how infection is recognized in *C. elegans*, several conserved signaling pathways are involved in controlling this

[6]corresponding author ewbank@ciml.univ-mrs.fr.
[7]authors contributed equally, *nipi-3* Genbank accession EU043523

innate immune response [6]. Among them, a p38 mitogen activated kinase (MAPK) pathway, involving the MAPK PMK-1, the MAPK kinase (MAPKK) SEK-1 and the MAPKK kinase (MAPKKK) NSY-1 is important for the resistance of *C. elegans* to infection by the Gram-negative bacterium *Pseudomonas aeruginosa* [7]. This pathway lies downstream of the TIR domain adapter TIR-1, ortholog of the human protein SARM [8]. In addition to a role in host defense, the TIR-1/NSY-1/SEK-1 cassette is also important for neuronal development. Interestingly, while the cassette acts downstream of the calcium/calmodulin-dependent kinase UNC-43 during development [9], *unc-43* is not required for resistance to *P. aeruginosa* [7].

In contrast to our current understanding of the response of *C. elegans* to bacterial infection, we know little about its anti-fungal innate immune defenses. One model pathogen is the nematode-specific fungus *Drechmeria coniospora*. Conidia of *D. coniospora* attach via adhesive knobs to the nematode cuticle and then form appressorial structures from which penetration tubes emerge. These pierce the cuticle and develop into trophic hyphae that traverse the epidermis, eventually colonizing the entire worm [10]. This natural fungal infection leads to the induction of a number of genes that encode conserved glycine- and tyrosine-rich antimicrobial peptides (AMPs) annotated as neuropeptide-like proteins (NLPs). We showed previously that the induction of two of these, *nlp-29* and *nlp-31* requires *tir-1* [11]. How *tir-1* is activated by fungal infection is unknown and it is unclear whether up-regulation of *nlp* gene expression is a consequence of pathogen recognition or part of a response to cellular damage associated with infection.

In the current study, we discovered that the *C. elegans* epidermis is capable of responding to physical injury. This response includes a wound healing mechanism and induction of *nlp-29* and *nlp-31* expression. We show that the up-regulation of AMP gene expression upon infection can be genetically separated from that upon injury, but that both responses converge on a common p38 MAPK pathway. Our results give insights into the possible origins and evolution of innate immunity.

Results

An *in vivo* reporter system for monitoring innate immune responses

To begin dissecting the innate immune response of *C. elegans* to fungal infection, we generated a strain carrying an integrated transgene (*frIs7*) with two constructs, the p*nlp-29*::GFP green fluorescent reporter that is induced upon infection in the epidermis [11], and a p*col-12*::dsRed red fluorescent reporter that is expressed constitutively in the epidermis, starting from the late L1 stage. The latter provides an internal control for the functional integrity of the epidermis and non-specific transgene silencing (Figure 1A,B). The analysis of large populations with the COPAS Biosort™ revealed a continuous distribution of fluorescence levels (Figure 1 C,D). While in a typical infection, the mean level of red fluorescence varied by less than 15% between non-infected and infected populations, for green fluorescence there was between a 3- and 8-fold increase (Figure 1C). Within a population, the green/red fluorescence ratio often spanned more than an order of magnitude, with a standard deviation exceeding 150% of the average in some cases. Even if the distribution is not Gaussian, the mean value for the fluorescence ratio is close to the median (Figure 1D) and therefore can be taken as a representative measure of reporter gene expression within the population. As discussed below, the individual variability in reporter gene expression, is no different from that measured for many quantitative phenotypes.

Physical injury induces *nlp-29* expression

Infection of *C. elegans* by *D. coniospora* involves a breach of the cuticle and disrupts epidermal cell integrity [10]. We therefore investigated whether physical wounding of the cuticle and

epidermis was sufficient to induce innate immune responses within the epidermis. Microinjection is a routine method to produce transgenic nematodes. Typically, an individual worm, immobilized on an agar pad, is pierced with a fine needle controlled by a micromanipulator. While large breaches in the epidermis cause an eversion of the internal tissues, when correctly performed, this procedure leaves no obvious mark (Suppl. Figure 1A). We found that wounding the epidermis in this way resulted in characteristic autofluorescent scars that formed rapidly and were visible for several days at the wound site. When we pricked the epidermis of adult animals on agar plates, by hand using microinjection needles, often no obvious damage was seen, although sometimes, a small amount of internal material leaked out. In both cases, wounding the epidermis provoked similar autofluorescent scars (Figures 2A–B & 3D–G).

We examined the survival of wounded worms under normal culture conditions. Although some 10% of the wounded worms died within two days after being injured, the remaining worms died at a rate that paralleled that of uninjured worms (Suppl. Figure 1B). The wounded worms also moved normally and showed no other outward signs of trauma. This suggests that wound healing efficiently restores normal physiology.

To cause more precise damage of epidermal cells, we used femtosecond laser pulses focused on the apical surface of the epidermis to create small wounds (Suppl. movie 1). Such laser wounding generally did not cause leakage of internal cytoplasm or fluid, but nevertheless resulted in scars 2–5 μm in diameter (Figure 2C), smaller but otherwise similar to those seen after needle wounding. Laser wound sites accumulated autofluorescent material within seconds of damage (Figure 2D; Suppl. movie 2).

Through ultrastructural analysis of laser wounds, we found that a continuous cuticle layer was re-established within 24 h of damage, suggesting that laser wounding causes a disruption of the epidermis and cuticle that is later repaired. At wound sites, we consistently observed thickening of basal layers of cuticle (Figure 2E–H) suggesting that wounds trigger local secretion of basal cuticle components as part of the barrier repair process.

Both needle and laser wounds induced p*nlp-29*::GFP expression with a similar time-course. GFP fluorescence was detected within 1 hour of injury, sustained for several hours and then declined (Figure 3A–G). While most experiments were conducted under standard culture conditions in the presence of bacteria, similar results were obtained when we wounded worms on bacteria-free plates (Suppl. Figure 1C). To our knowledge, these are the first indications that *C. elegans* is able to respond transcriptionally to physical injury.

Defects in the epidermis induce *nlp-29* expression

We wondered whether mutants with a defect in the cuticle or epidermis would also show a changed level of p*nlp-29*::GFP expression. Worms carrying a dominant mutation in the cuticle collagen gene *rol-6* exhibited a strong constitutive expression of green fluorescence (results not shown). In *C. elegans*, almost all of the epidermis is a single multinucleate syncytium called hyp7. When we looked at p*nlp-29*::GFP expression in *eff-1* mutant animals that exhibit abnormal hyp7 cell fusions [12,13], we also saw a high level of GFP expression, often most intense in non-fused cells (Figure 3H,I). Thus developmental defects and tissue damage lead to the up-regulation of AMP expression.

A conserved p38 MAPK pathway controls AMP gene expression

We have previously shown that infection-induced expression of p*nlp-29*::GFP is severely compromised upon RNAi of *tir-1* [11]. By performing RNAi on the different *tir-1* isoforms (Suppl. Figure 2), we established that *tir-1b* is required for the infection-induced expression

of *nlp-29*, as well as for the response of *C. elegans* to wounding (Figure 4A). Accordingly, in mutant worms homozygous for *tir-1* loss-of-function alleles which affect only the *tir-1a, c* and *e* isoforms, but not *tir-1b* or *d*, we observed no change in constitutive or induced expression of p*nlp-29*::GFP, whereas in the *tir-1(tm3036)* mutant, which affects all isoforms, induction of p*nlp-29*::GFP was blocked (Figure 4B–C,Suppl. Figure 2). *tir-1* acts upstream of the *nsy-1/sek-1/pmk-1* p38 pathway to control resistance to the intestinal pathogen *P. aeruginosa* [8]. We therefore assayed the effect of abrogation of these genes on the expression of p*nlp-29*::GFP. In *nsy-1*, *sek-1* or *pmk-1* mutants there was a marked decrease in p*nlp-29*::GFP expression following both infection and wounding (Figure 4C–E, results not shown).

During neuronal development, the *tir-1*/*nsy-1/sek-1* cascade acts genetically downstream of the CaMK II *unc-43* [9,14]. We found that p*nlp-29*::GFP expression and induction after infection was unaltered in an *unc-43* loss-of-function mutant (Figure 4F). Thus, just as it is not required for the response to *P. aeruginosa* infection [7], *unc-43* appears not to be involved in the response to *D. coniospora*. Similarly, abrogation of *unc-16*, which encodes a scaffold protein that interacts with SEK-1 [15], had no effect on constitutive or infection-induced expression of p*nlp-29*::GFP. Further, *jkk-1*, *kgb-1* or *jnk-1* that are elements of JNK MAPK cascades that play an important role in the response of *C. elegans* to stress [16,17] were found to be dispensable for p*nlp-29*::GFP expression (Figure 4F and data not shown). In a *mek-1* mutant background, there was a partial reduction in the induction of p*nlp-29*::GFP (Figure 4F). Therefore, *mek-1*, which encodes a MKK7 homolog, may have a role in the activation of *pmk-1*, as previously described in the context of *P. aeruginosa* infection [16]. The predominant pathway controlling p*nlp-29*::GFP expression does, however, involve the NSY-1/SEK-1/PMK-1 cassette.

The p38 MAPK pathway acts cell-autonomously in the epidermis

The p38 pathway acts cell-autonomously during neuronal development [18] and in the adult intestine to protect *C. elegans* from oxidative stress [19]. We tested whether the p38 pathway is required in the epidermis to control AMP gene induction. Expressing *sek-1* in the epidermis under the control of the *col-12* promoter was more than sufficient to restore p*nlp-29*::GFP expression in a *sek-1* mutant (Figure 4G). When the transgene was transferred to a wild-type background, the transgenic animals had an increased constitutive and induced fluorescence, while in a *pmk-1* background, there was essentially no observable fluorescence (Figure 6F). These results strongly suggest that SEK-1 and by extension the entire p38 pathway acts cell-autonomously in the epidermis to control AMP expression.

A genetic screen for genes controlling *nlp-29* expression

We next screened for mutants that had a normal level of p*col-12*::dsRed expression but that were unable to activate p*nlp-29*::GFP expression after infection (see Experimental Procedures). From an initial screen of 10,000 haploid genomes, we recovered six Nipi (No Induction of Peptide after *Drechmeria* Infection) mutants. The six *nipi* mutations are recessive and were assigned to five complementation groups. Of the five, four affected p*nlp-29*::GFP expression following both infection and wounding (Figure 5A; NP, unpublished data). The mutants *nipi-1* (*fr1* and *fr3*) LGIV, *nipi-2*(*fr2*) LGX and *nipi-3*(*fr4*) LGX showed the most penetrant phenotypes. Complementation tests with available mutants suggested that these 3 *nipi* mutants do not correspond to known components of the *C. elegans* p38 MAPK pathway.

nipi-3 a Tribbles-like kinase is required in the response to infection

We focused on *nipi-3(fr4)*, in which the infection-induced up-regulation of p*nlp-29*::GFP was essentially abolished, but that still responded strongly to injury (Figure 5A). As expected, in *nipi-3* mutants we observed an abrogation of *nlp-29* mRNA induction upon infection but not wounding, as measured by qRT-PCR (Figure 5B). We found that the expression of a second

AMP gene, *nlp-31*, which is induced by *D. coniospora* infection [11], was also up-regulated upon wounding. Only the infection response was affected in the *nipi-3* mutant (Figure 5B). These results suggest that *nipi-3(fr4)* is specifically involved in regulating the transcriptional response to infection.

We identified *nipi-3* as K09A9.1, predicted to encode a protein serine/theronine kinase (Figure 5D). When compared to human proteins, NIPI-3 is most similar to Tribbles homolog 1 (TRIB1/hTribbles), especially in the kinase domain (residues 237–461; Figure 5E). Among *C. elegans* proteins, NIPI-3′s most extended similarity is to the uncharacterized hypothetical protein ZK524.4 and to UNC-43. The region of conservation between NIPI-3 and UNC-43 spans part of the kinase domain and some 100 C-terminal residues (Suppl. Figure 3A). The *nipi-3(fr4)* mutation is in the kinase domain changing a conserved hydrophobic residue to an asparagine (I307N; Figure 5D&E). The mutated residue is spatially separate from the substrate binding pocket, catalytic site, ATP-binding and activation loops (Suppl. Figure 3B).

nipi-3 mutants also exhibited a temperature-sensitive Dpy phenotype: at 25°C *nipi-3* mutants were 20% shorter on average than wild-type worms (Suppl. Figure 4). Reintroduction of a 3.6 kb wild-type genomic DNA fragment comprising the coding and 5′ and 3′ sequences fully rescued the *nipi-3(fr4)* mutant phenotypes (Figure 5D, 6E; Suppl. Figure 4). Abrogation of *nipi-3* function through RNAi recapitulated the effects on p*nlp-29*::GFP expression seen in a *nipi-3(fr4)* mutant (Figure 5C) and did not provoke any other obvious phenotype (e.g. embryonic or larval lethality, uncoordinated movement). Taken together these results suggest the *fr4* mutation causes a loss of *nipi-3* function.

To assay for a direct role of *nipi-3* in controlling fungal resistance, we compared the survival of wild-type and mutant worms after *D. coniospora* infection. There was a significant reduction in the resistance of the *nipi-3* mutants, as well as in *pmk-1(km25)* and *tir-1(tm3036)* mutants. These mutants also had a reduced lifespan on the *E. coli* strain OP50 (Suppl. Figure 5). This precludes definitively assigning a role in anti-fungal resistance to *nipi-3*.

Using a GFP transcriptional reporter construct, we found that *nipi-3* is expressed in the epidermis as well as in the pharynx and intestine, in a subset of head neurons and motoneurons, and in the PLM and CAN neurons (Figure 6A–D, results not shown). When *nipi-3* was specifically expressed in the epidermis, under the control of the *col-12* promoter, the induction of p*nlp-29*::GFP after infection was restored to wild-type levels in a fraction (ca. 1/5) of the transgenic worms. On the other hand, intestinal expression of *nipi-3*, under the control of the *mlt-2* promoter, completely failed to rescue the mutant phenotype (Figure 6G–N; Suppl. Figure 6). Thus, *nipi-3* is a new component of innate immune signaling in *C. elegans* and acts in the epidermis to control AMP expression after infection.

NIPI-3 bears some similarity to UNC-43, a kinase required for establishing the unique identity of the two AWC chemosensory neurons [14]. Unlike *unc-43*, *nipi-3* is not required for asymmetric gene expression in the AWC neurons (data not shown). UNC-43 forms a complex with TIR-1 and NSY-1 and signals through SEK-1 [9]. In the presence of the p*col-12::sek-1* transgene, the level of constitutive expression of p*nlp-29*::GFP in a *nipi-3* mutant background was elevated, and similar to that in wild-type worms. In contrast, in a *pmk-1* mutant background, the level of expression was much lower (Figure 6F). These results imply that *nipi-3* does not act downstream of *sek-1*. After infection, in the *nipi-3*;p*col-12::sek-1* strain there was a two-fold increase in the expression of p*nlp-29*::GFP. As discussed below, these results are consistent with *nipi-3* acting upstream of *sek-1*.

Discussion

Continuous Distribution of a Quantitative Signalling Readout

The use of the Biosort allows the level of fluorescent reporter gene expression to be measured in single worms. We observed large differences in p*nlp-29*::GFP expression between infected individuals. This may in part reflect variation in the precise course of the infection, determined among other things by the density and location of spore attachment, and the initial level of AMP expression. The individual variation recorded for the constitutive expression of p*nlp-29*::GFP in uninfected worms may be surprising, especially since *C. elegans* is a self-fertilizing hermaphrodite species, and the individuals in a population are genetically identical. Other studies, measuring the expression of other *C. elegans* reporter genes with the Biosort have revealed a similar range of expression levels [20,21]. This type of stochastic variation appears to be a widespread phenomenon. Even in yeast, a wide range of values is seen for the expression of the same gene in different individual cells under identical conditions [22,23]. In yeast, noise in expression levels generally scales with protein abundance. Exceptions to this rule are the stress response proteins, induced under stressful conditions [24]. It has been proposed that this phenotypic variability might enable cells to adapt better to changing environments [25]. It is possible that the observed variability in p*nlp-29*::GFP expression also plays an adaptive role. Despite this variability, and regardless of any function, the p*nlp-29*::GFP transgene constitutes a useful tool for dissecting innate immune signalling pathways.

An epidermal wounding response in *C. elegans*

We used the p*nlp-29*::GFP reporter to demonstrate for the first time that *C. elegans* responds to physical injury of the epidermis by up-regulating AMP gene expression. Since we show elsewhere (Pujol et al. submitted) that increased AMP gene expression renders *C. elegans* more resistant to infection, this mechanism may help worms counter septic injuries that occur in nature. It has been recently shown that in mammalian skin AMP gene expression is induced by sterile injury [26]. Thus protection of the epidermis from infection in such high-risk situations may be a conserved aspect of animal physiology. In Drosophila, clean wounding causes melanization at the wound site [27]. The *C. elegans* genome encodes tyrosinases that may be evolutionarily related to the prophenoloxidases responsible for melanin biosynthesis in invertebrates [28]. But when we injured the epidermis of *C. elegans*, we observed no obvious melanin deposition, but rather the almost immediate accumulation at the wound site of autofluorescent material, followed by the repair of the extracellular matrix of the barrier epithelium. Possible triggers for these wound healing and innate immune responses, include rupture of the epidermal apical plasma membrane, or the disruption of contacts between the epidermis and cuticle.

The response to fungal infection is distinct from the epidermal wounding response

While the repair of the barrier epidermis itself can be considered as an innate immune response in that it protects the organism from opportunistic infection, the isolation of the *nipi-3(fr4)* mutant shows that in *C. elegans* separable signalling cascades control gene expression after infection and wounding. Thus this strong loss of function mutant shows a limited induction of the two AMP genes *nlp-29* or *nlp-31* after infection but a near-normal induction of the same two genes following wounding. In the presence of artificially high levels of *sek-1*, even in a *nipi-3* background, there is sufficient activation of the pathway to lead to high expression of p*nlp-29*::GFP after infection. Since in the *pmk-1;*p*col-12::sek-1* strain, there is no such elevated p*nlp-29*::GFP expression even after infection, it would appear that the p38 MAPK is a key regulator of *nlp-29*, and consequently that *nipi-3* acts through this pathway.

Conservation of MAPK signaling modules

Although the responses to *D. coniospora* and injury can be genetically distinguished, they do converge on the TIR-domain adapter protein TIR-1B and downstream p38 MAPK pathway components. Taken together with the results of our epistasis experiments, this suggests that *nipi-3* acts upstream of *tir-1*. By analogy with the role of UNC-43 in neurons [9], we speculate that NIPI-3 functions as a direct activator of TIR-1B in the epidermis. This would imply that an infection-associated signal exists upstream of NIPI-3. Whatever the mechanisms involved in triggering the infection-specific epidermal response in *C. elegans*, it is striking to note that the same signaling cassette (TIR-1/NSY-1/SEK-1) is used in at least three different contexts (Figure 7). This parallels the situation in the yeast *Saccharomyces cerevisiae*, wherein the NSY-1-like MAP3K Ste11p acts in three different biological processes [29]. Interestingly, Ste11p, and Ste50p, its upstream partner possess SAM domains, like TIR-1 (Figure 7). Indeed, close inspection of the NSY-1 sequence reveals that it contains a divergent SAM domain, within a larger conserved motif, present in the vertebrate proteins, ASK1 and ASK2 (Suppl. Figure 7). Importantly, in mice, upon stimulation by lipopolysaccharide, ASK1 selectively activates the p38 pathway [30]. Moreover, ASK1 regulates the expression of β-defensins and LL37, AMPs produced by human epidermis, in a p38-dependent manner [31]. These findings suggest that SAM domains may have played an ancestral role in innate immune signaling that was complemented by the recruitment of TIR domain-containing proteins. Additionally, our results give strong support to the idea that part of vertebrate innate immunity has its origins in MAPK signaling pathways that arose early in evolution to conserve cellular homeostasis. The finding that NIPI-3, a protein kinase with a catalytic domain that is most similar to the human Tribbles homolog 1 is involved in the response to infection is particularly interesting since this protein has been identified as acting in the p38 pathway in vertebrates [32,33], thus extending the number of proteins potentially involved in this conserved signaling cascade.

The activation of *nlp-29* and *nlp-31* by wounding suggests that in *C. elegans*, as perhaps in vertebrates [34], tissue damage triggers an innate immune response. The *nipi-3* gene, however, defines a genetically distinct response to infection. Our results thus support the existence of a pathogen-specific reaction, in addition to a non-specific protective response. Both share components of a p38-signaling cascade; the former may have evolved more recently. In conclusion, the current work advances our knowledge of host defenses in the nematode *C. elegans* and contributes to the debate on the origins and evolution of innate immunity.

Experimental Procedures

nipi-3 isolation, cloning and rescue

We mutagenized *wt;frIs7* worms with EMS using standard procedures [35]. Synchronized F2 worms were infected at the L4 stage with *D. coniospora*. After 24 h at 25°C, we screened, either automatically with the Biosort, or visually and manually, for worms that failed to show an elevated level of GFP expression after *D. coniospora* infection. *nipi-3(fr4)* was mapped through standard genetic and SNP mapping by analysis of 360 recombinants with the strain CB4856, to a 145 kb region left of *lin-15* on LGX, containing 21 predicted genes. Sequencing of the gene K09A9.1 revealed a single point mutation in *nipi-3* mutants, a T to A transition (flanking sequences TGAAAACGACGTGATGAGTA and CTACCAAAAGGTTGTGGAGA). A full-length cDNA was generated and sequenced from wild-type worms, leading to a modification of the gene structure predicted in Wormbase (WS180), see Genbank accession number EU043523. The *nipi-3(fr4)* allele changes an isoleucine to an asparagine at position 307 of the predicted protein sequence. To confirm the identity of *nipi-3*, the K09A9.1 gene with 1426 bp upstream and 1753 bp downstream was amplified by PCR with the primers JEP963 and JEP964 and microinjected (at 5 ng/μl with 80 ng/μl pB*unc-53*::GFP [36]) into *nipi-3(fr4);frIs7* mutant worms. Two independent lines IG581

nipi-3(fr4);frIs7;frEx195 and IG580 *nipi-3(fr4);frIs7;frIs10* were generated; the latter is a spontaneous integrant.

Supplementary Material

Refer to Web version on PubMed Central for supplementary material.

Acknowledgements

We thank Y. Duverger and S. Scaglione for worm sorting, M. Fallet for help with image processing, Z. Wu for assistance with the femtosecond laser, H. Agherbi for help with integration of *frIs7*, O. Zugasti for generating some transgenic strains. Worm sorting analyses were carried out using the facilities of the Marseille-Nice Genopole®. Some nematode strains were provided by the *Caenorhabditis* Genetics Center, which is funded by the NIH National Center for Research Resources (NCRR), or by the National Bioresource Project coordinated by S. Mitani. This work was funded by institutional grants from INSERM and the CNRS, the French Ministry of Research *Programme de Microbiologie*, ACI BDPI and BCMS, the RNG, ANR, the NSF (OISE 0726131) and the French Foreign Ministry (France Berkeley Fund). Y.J. is an Investigator of the Howard Hughes Medical Institute. The Ewbank lab is an FRM équipe labellisée.

References

1. Mallo GV, Kurz CL, Couillault C, Pujol N, Granjeaud S, Kohara Y, Ewbank JJ. Inducible antibacterial defense system in *C. elegans*. Curr Biol 2002;12:1209–1214. [PubMed: 12176330]
2. O'Rourke D, Baban D, Demidova M, Mott R, Hodgkin J. Genomic clusters, putative pathogen recognition molecules, and antimicrobial genes are induced by infection of *C. elegans* with *M. nematophilum*. Genome Res 2006;16:1005–1016. [PubMed: 16809667]
3. Troemel ER, Chu SW, Reinke V, Lee SS, Ausubel FM, Kim DH. p38 MAPK Regulates Expression of Immune Response Genes and Contributes to Longevity in *C. elegans*. PLoS Genetics 2006;2:e183. [PubMed: 17096597]
4. Shapira M, Hamlin BJ, Rong J, Chen K, Ronen M, Tan MW. A conserved role for a GATA transcription factor in regulating epithelial innate immune responses. Proc Natl Acad Sci U S A 2006;103:14086–14091. [PubMed: 16968778]
5. Wong D, Bazopoulou D, Pujol N, Tavernarakis N, Ewbank JJ. Genome-wide investigation reveals pathogen-specific and shared signatures in the response of *C. elegans* to infection. Genome Biol 2007;8:R194. [PubMed: 17875205]
6. Ewbank, JJ. Signaling in the Immune Response. WormBook Volume. 2006. The *C. elegans* Research Community, ed. (http://www.wormbook.org)
7. Kim DH, Feinbaum R, Alloing G, Emerson FE, Garsin DA, Inoue H, Tanaka-Hino M, Hisamoto N, Matsumoto K, Tan MW, Ausubel FM. A conserved p38 MAP kinase pathway in *Caenorhabditis elegans* innate immunity. Science 2002;297:623–626. [PubMed: 12142542]
8. Liberati NT, Fitzgerald KA, Kim DH, Feinbaum R, Golenbock DT, Ausubel FM. Requirement for a conserved Toll/interleukin-1 resistance domain protein in the *Caenorhabditis elegans* immune response. Proc Natl Acad Sci U S A 2004;101:6593–6598. [PubMed: 15123841]
9. Chuang CF, Bargmann CI. A Toll-interleukin 1 repeat protein at the synapse specifies asymmetric odorant receptor expression via ASK1 MAPKKK signaling. Genes Dev 2005;19:270–281. [PubMed: 15625192]
10. Dijksterhuis J, Veenhuis M, Harder W. Ultrastructural study of adhesionand initial stages of infection of the nematode by conidia of *Drechmeria coniospora*. Mycological research 1990;94:1–8.
11. Couillault C, Pujol N, Reboul J, Sabatier L, Guichou JF, Kohara Y, Ewbank JJ. TLR-independent control of innate immunity in *Caenorhabditis elegans* by the TIR domain adaptor protein TIR-1, an ortholog of human SARM. Nat Immunol 2004;5:488–494. [PubMed: 15048112]
12. Shemer G, Suissa M, Kolotuev I, Nguyen KC, Hall DH, Podbilewicz B. EFF-1 is sufficient to initiate and execute tissue-specific cell fusion in *C. elegans*. Curr Biol 2004;14:1587–1591. [PubMed: 15341747]

13. Mohler WA, Shemer G, del Campo JJ, Valansi C, Opoku-Serebuoh E, Scranton V, Assaf N, White JG, Podbilewicz B. The type I membrane protein EFF-1 is essential for developmental cell fusion. Dev Cell 2002;2:355–362. [PubMed: 11879640]
14. Sagasti A, Hisamoto N, Hyodo J, Tanaka-Hino M, Matsumoto K, Bargmann CI. The CaMKII UNC-43 activates the MAPKKK NSY-1 to execute a lateral signaling decision required for asymmetric olfactory neuron fates. Cell 2001;105:221–232. [PubMed: 11336672]
15. Byrd DT, Kawasaki M, Walcoff M, Hisamoto N, Matsumoto K, Jin Y. UNC-16, a JNK-signaling scaffold protein, regulates vesicle transport in *C. elegans*. Neuron 2001;32:787–800. [PubMed: 11738026]
16. Kim DH, Liberati NT, Mizuno T, Inoue H, Hisamoto N, Matsumoto K, Ausubel FM. Integration of *Caenorhabditis elegans* MAPK pathways mediating immunity and stress resistance by MEK-1 MAPK kinase and VHP-1 MAPK phosphatase. Proc Natl Acad Sci U S A 2004;101:10990–10994. [PubMed: 15256594]
17. Mizuno T, Hisamoto N, Terada T, Kondo T, Adachi M, Nishida E, Kim DH, Ausubel FM, Matsumoto K. The *Caenorhabditis elegans* MAPK phosphatase VHP-1 mediates a novel JNK-like signaling pathway in stress response. Embo J 2004;23:2226–2234. [PubMed: 15116070]
18. Tanaka-Hino M, Sagasti A, Hisamoto N, Kawasaki M, Nakano S, Ninomiya-Tsuji J, Bargmann CI, Matsumoto K. SEK-1 MAPKK mediates Ca^{2+} signaling to determine neuronal asymmetric development in *Caenorhabditis elegans*. EMBO Rep 2002;3:56–62. [PubMed: 11751572]
19. Inoue H, Hisamoto N, An JH, Oliveira RP, Nishida E, Blackwell TK, Matsumoto K. The *C. elegans* p38 MAPK pathway regulates nuclear localization of the transcription factor SKN-1 in oxidative stress response. Genes Dev 2005;19:2278–2283. [PubMed: 16166371]
20. Cardoso C, Couillault C, Mignon-Ravix C, Millet A, Ewbank JJ, Fontes M, Pujol N. XNP-1/ATR-X acts with RB, HP1 and the NuRD complex during larval development in *C. elegans*. Dev Biol 2005;278:49–59. [PubMed: 15649460]
21. Rea SL, Wu D, Cypser JR, Vaupel JW, Johnson TE. A stress-sensitive reporter predicts longevity in isogenic populations of *Caenorhabditis elegans*. Nat Genet 2005;37:894–898. [PubMed: 16041374]
22. Attfield PV, Choi HY, Veal DA, Bell PJ. Heterogeneity of stress gene expression and stress resistance among individual cells of *Saccharomyces cerevisiae*. Mol Microbiol 2001;40:1000–1008. [PubMed: 11401706]
23. Ryley J, Pereira-Smith OM. Microfluidics device for single cell gene expression analysis in *Saccharomyces cerevisiae*. Yeast 2006;23:1065–1073. [PubMed: 17083143]
24. Bar-Even A, Paulsson J, Maheshri N, Carmi M, O'Shea E, Pilpel Y, Barkai N. Noise in protein expression scales with natural protein abundance. Nat Genet 2006;38:636–643. [PubMed: 16715097]
25. Barkai N, Shilo BZ. Variability and robustness in biomolecular systems. Mol Cell 2007;28:755–760. [PubMed: 18082601]
26. Sorensen OE, Thapa DR, Roupe KM, Valore EV, Sjobring U, Roberts AA, Schmidtchen A, Ganz T. Injury-induced innate immune response in human skin mediated by transactivation of the epidermal growth factor receptor. J Clin Invest 2006;116:1878–1885. [PubMed: 16778986]
27. De Gregorio E, Han SJ, Lee WJ, Baek MJ, Osaki T, Kawabata S, Lee BL, Iwanaga S, Lemaitre B, Brey PT. An immune-responsive Serpin regulates the melanization cascade in *Drosophila*. Dev Cell 2002;3:581–592. [PubMed: 12408809]
28. Cerenius L, Soderhall K. The prophenoloxidase-activating system in invertebrates. Immunol Rev 2004;198:116–126. [PubMed: 15199959]
29. Schwartz MA, Madhani HD. Principles of MAP kinase signaling specificity in *Saccharomyces cerevisiae*. Annu Rev Genet 2004;38:725–748. [PubMed: 15568991]
30. Matsuzawa A, Saegusa K, Noguchi T, Sadamitsu C, Nishitoh H, Nagai S, Koyasu S, Matsumoto K, Takeda K, Ichijo H. ROS-dependent activation of the TRAF6-ASK1-p38 pathway is selectively required for TLR4-mediated innate immunity. Nat Immunol 2005;6:587–592. [PubMed: 15864310]
31. Sayama K, Komatsuzawa H, Yamasaki K, Shirakata Y, Hanakawa Y, Ouhara K, Tokumaru S, Dai X, Tohyama M, Ten Dijke P, Sugai M, Ichijo H, Hashimoto K. New mechanisms of skin innate immunity: ASK1-mediated keratinocyte differentiation regulates the expression of beta-defensins, LL37, and TLR2. Eur J Immunol 2005;35:1886–1895. [PubMed: 15864780]

32. Kiss-Toth E, Bagstaff SM, Sung HY, Jozsa V, Dempsey C, Caunt JC, Oxley KM, Wyllie DH, Polgar T, Harte M, O'Neill LA, Qwarnstrom EE, Dower SK. Human tribbles, a protein family controlling mitogen-activated protein kinase cascades. J Biol Chem 2004;279:42703–42708. [PubMed: 15299019]

33. Kiss-Toth E, Wyllie DH, Holland K, Marsden L, Jozsa V, Oxley KM, Polgar T, Qwarnstrom EE, Dower SK. Functional mapping and identification of novel regulators for the Toll/Interleukin-1 signalling network by transcription expression cloning. Cell Signal 2006;18:202–214. [PubMed: 15990277]

34. Matzinger P. Friendly and dangerous signals: is the tissue in control? Nat Immunol 2007;8:11–13. [PubMed: 17179963]

35. Wood, WB., editor. The nematode *Caenorhabditis elegans*. Plainview, N. Y: Cold Spring Harbor Laboratory Press; 1988.

36. Stringham E, Pujol N, Vandekerckhove J, Bogaert T. *unc-53* controls longitudinal migration in *C. elegans*. Development 2002;129:3367–3379. [PubMed: 12091307]

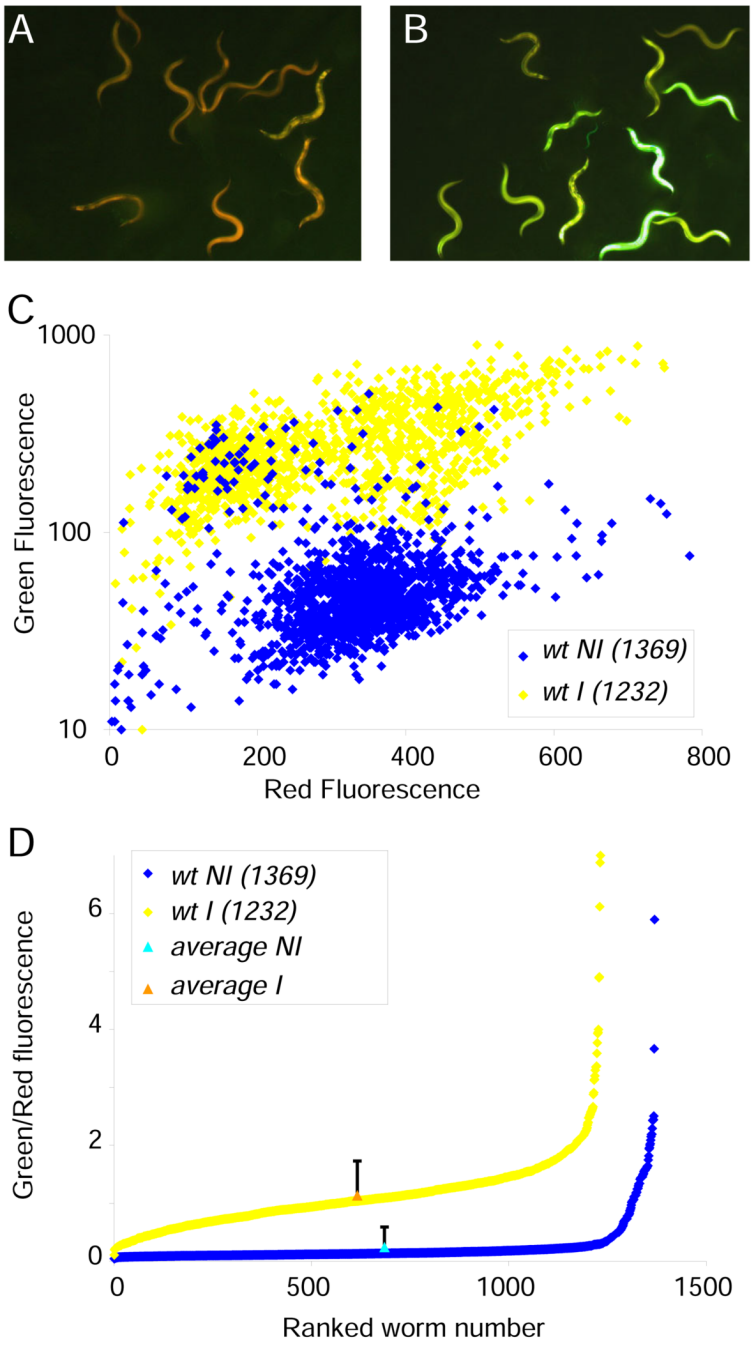

Figure 1. The p*nlp-29*::GFP reporter is induced by *Drechmeria coniospora*

Control *wt;frIs7* worms (**A**) and worms 24 h after infection (**B**). Red and green fluorescence is visualized simultaneously. **C Quantification of fluorescence** of infected (yellow) and non-infected (blue) worms. The mean values for green and red fluorescence (in arbitrary, but constant units for each colour) for the uninfected and infected populations were 59 and 287 (green) and 331.5 and 295.0 (red), respectively. **D Continuous distribution of fluorescence levels in the population**. The analysis of large numbers of individuals revealed a continuous distribution of fluorescence levels, with the median value for the fluorescence ratio (green/red) being close to the mean (triangles). Although there was an extremely broad range of values for individuals (from 4 to 589, and 11 to 700 in arbitrary units for 1369 non-infected and 1232

infected worms, respectively, in this experiment), leading to high standard deviations (157% and 54% of the mean values, respectively; shown as error bars with the mean at the median position), and noise (variance/mean^2, 2.4 and 0.3, respectively). Due to the nature of the distribution, standard deviations are not an informative parameter and are not shown on subsequent figures using the Biosort.

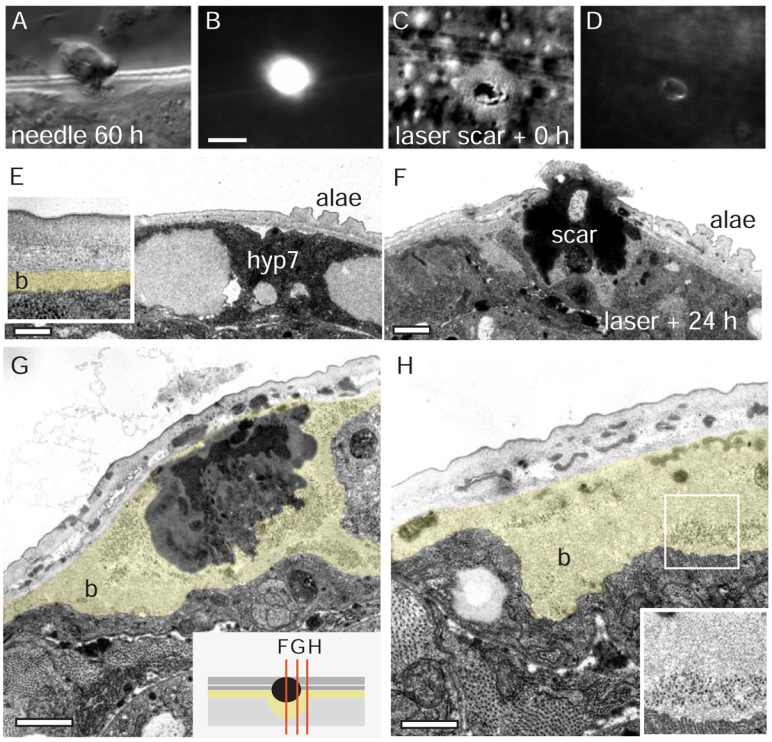

Figure 2. Needle and laser wounding of the epidermis cause scar formation and local cuticle synthesis

A–D Epidermal scars in wild type (N2) 60 h after needle wound (A,B) and immediately after femtosecond laser wound (C,D); DIC image (panels A, C) and epifluorescence (GFP long pass filter, panels B,D). The autofluorescent material accumulates at the wound immediately (see Suppl. Movies). Scale 10 μm. **E–H** Ultrastructural analysis of scar and cuticle synthesis at epidermal wounds. The lateral epidermis just ventral to the alae was damaged internally by aiming for the PLM axonal process (in the *zdIs5* strain) and cutting it with MHz femtosecond laser. F–H wounded and unwounded (E) sides of the same animal 24 h post wounding. The innermost (basal) layer of cuticle (b) is immediately adjacent to the epidermis hyp7 and is approximately 100 nm thick in unwounded epidermis (b, coloured in inset, E). Surrounding the electron dense material of the scar, the basal layer is up to 20 times thicker than in unwounded cuticle, and contains ribosome-sized electron dense particles (inset, H). Images are all from one animal, sections in F, G, and H are 1.3 μm apart (schematic in inset, G). Scale bar 2 μm.

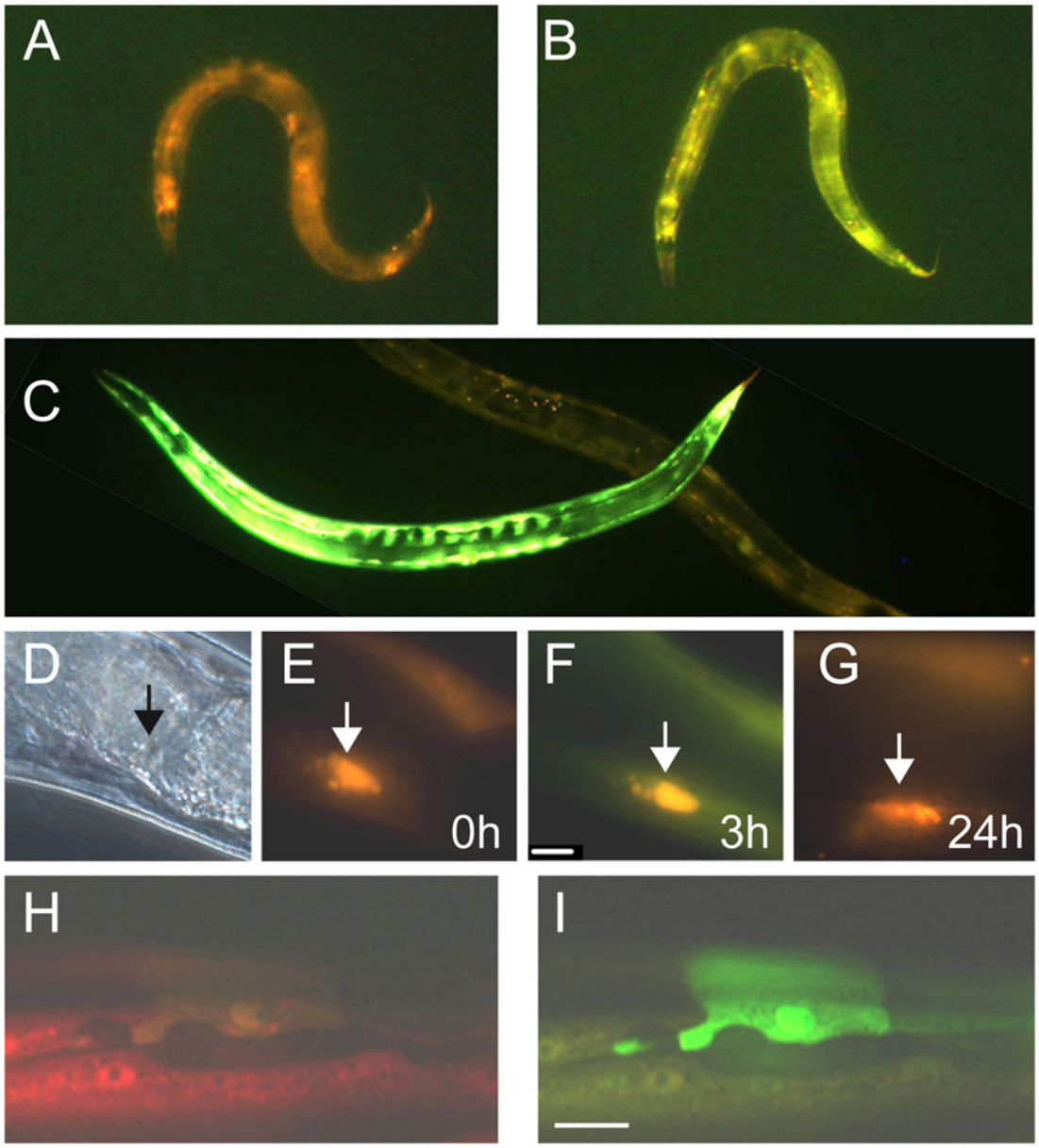

Figure 3. Epidermal damage induce p*nlp-29*::GFP

An individual *wt;frIs7* worm before (**A)** and 2 h after needle wounding (**B**). **C** An individual that has been wounded with a laser 5 h previously is lying above a mock-wounded worm. **D–G** An individual worm viewed by DIC (D) or epifluorescence (E) microscopy just after needle wounding. The arrowhead marks the wound site. The same worm 3 hours (F) or 24 hours (G) after wounding. **H & I** Part of the epidermis of an *eff-1(hy21);frIs7* worm. One unfused hyp7 cell shows strong GFP fluorescence (I). With the exception of D (DIC) and H (epifluorescence using a red filter to visualize p*col-12*:DsRed only), in all images, red and green fluorescence are visualized simultaneously.

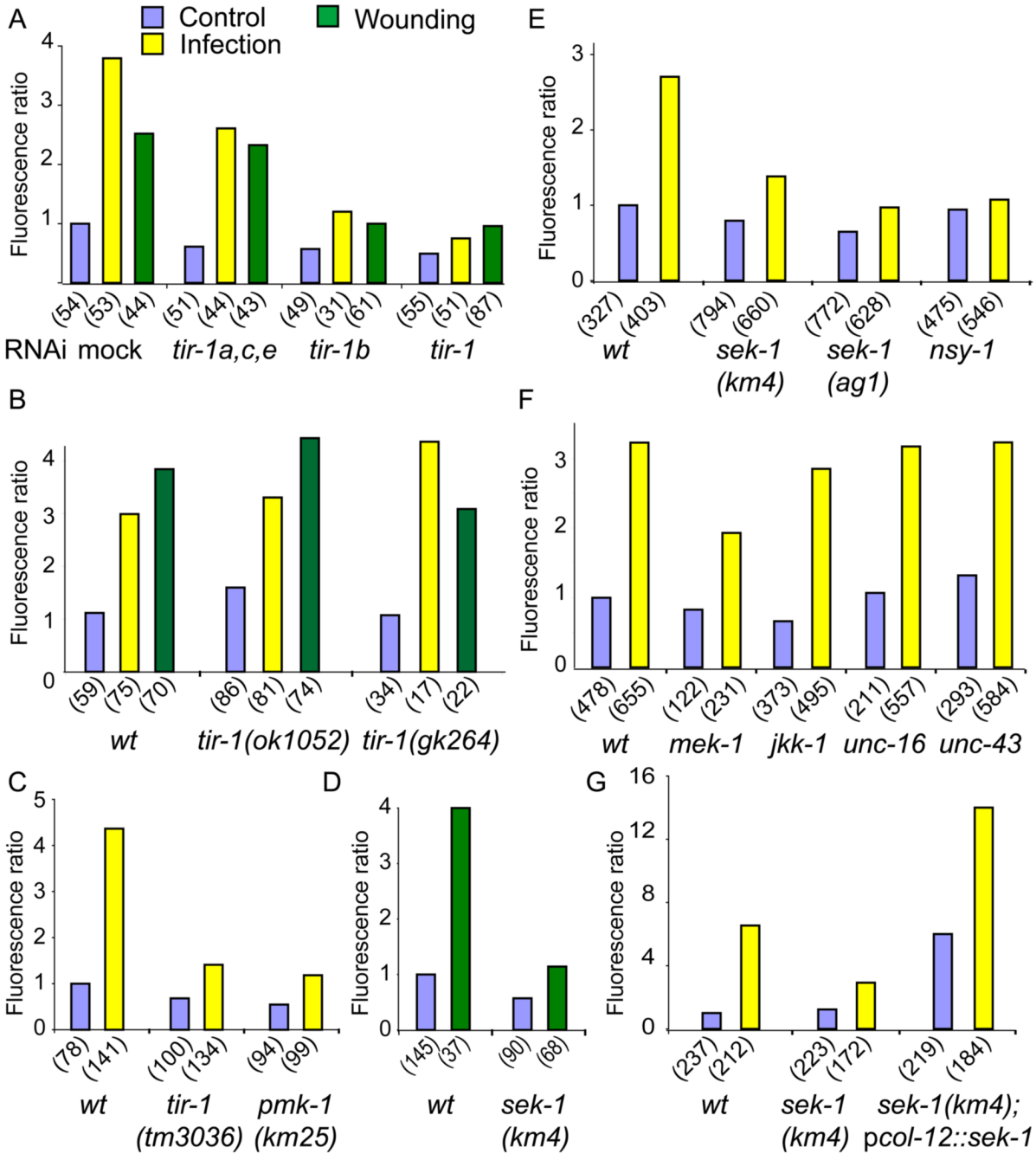

Figure 4. *nlp-29* induction after infection and injury is dependent on the TIR-1B/p38 pathway

Quantification with the Biosort of the normalized fluorescence ratio of worms carrying the *frIs7* transgene. **A** RNAi was used to target the different *tir-1* isoforms, and fluorescence measured 24 h post-infection (yellow) or 6 h after wounding (green) and compared to control worms (blue). **B** Mutants affecting the long *tir-1* isoforms (*ok1052*) and (*gk264*) have an essentially wild type phenotype. **C–F** Different mutants were analyzed after infection and wounding: *sek-1(ag1)*, *sek-1(km4)*, *nsy-1(ky397)*, *pmk-1(km25)*, *mek-1(ks54)*, *jkk-1(km2)*, *unc-16(ju146)* and *unc-43(n498n1186)*. **G** Over-expression of *sek-1* in the epidermis, under the control of the *col-12* promoter provokes high fluorescence ratios in *sek-1* mutants. The number of worms in each sample is given in parentheses.

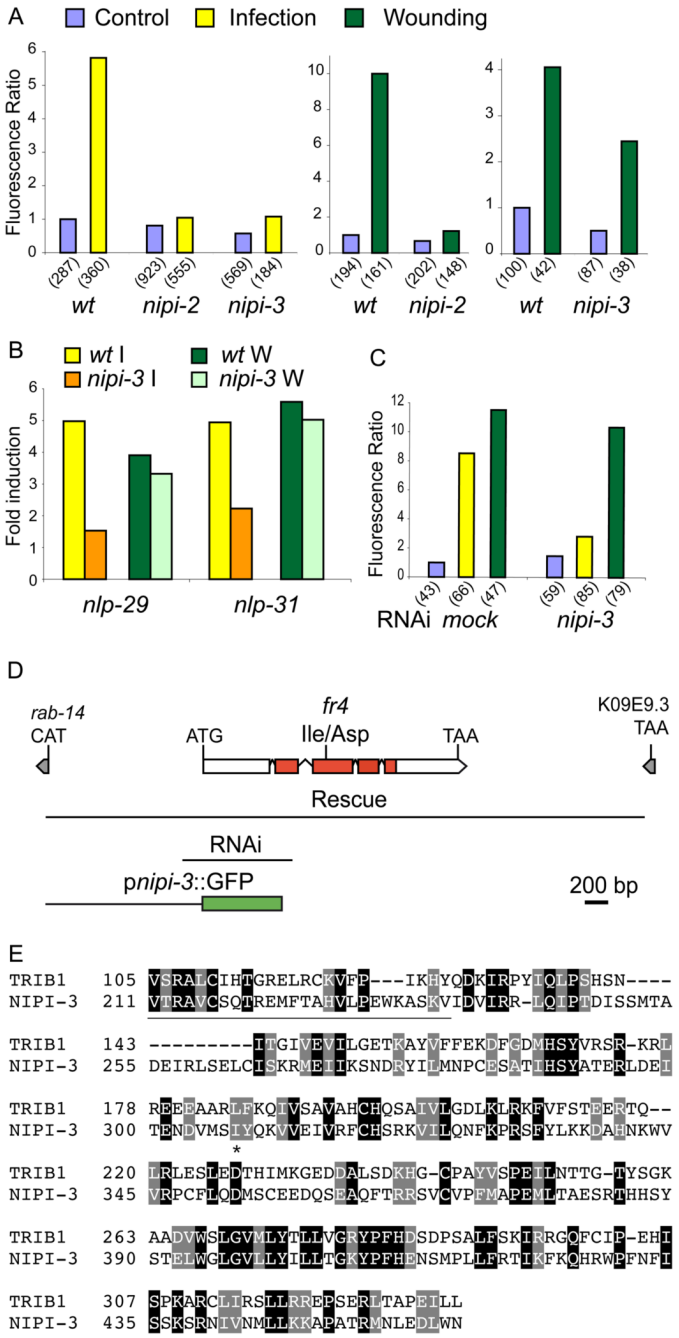

Figure 5. *nipi-3* encodes a kinase required for the induction of *nlp-29* and *nlp-31* after infection but not after wounding A

Quantification with the Biosort of the normalized fluorescence ratio of transgenic worms carrying the *frIs7* transgene 24 h post-infection (yellow; left panel) or 6 h after wounding (green; right panels) in *wt, nipi-2(fr2)* and *nipi-3(fr4)* mutant worms compared to controls (blue). **B** Quantification by qRT-PCR of *nlp-29* and *nlp-31* mRNA in wild-type and *nipi-3* mutant worms after infection (yellow and orange, respectively) or wounding (green and lime, respectively). **C** Quantification with the Biosort of the normalized fluorescence ratio of *wt;frIs7* worms 24 h post-infection (yellow) or 6 h after wounding (green) compared to controls (blue), following mock RNAi or RNAi of *nipi-3*. **D** Structure of the *nipi-3* locus. The location

of the *fr4* mutation is shown relative to the exon/intron structure of *nipi-3*; the red shading in 4 exons represents the kinase domain. Grey boxes represent the predicted 5′ and 3′-most exons of the neighbouring upstream and downstream genes, respectively. The first line below the gene indicates the extent of the genomic fragment used to rescue the mutant phenotype; the next line (labelled RNAi), that used for RNAi and the third line, the promoter region used to drive the expression of GFP in the reporter construct. **E** The *nipi-3* gene encodes a protein with similarity to human Tribbles homolog 1 (TRIB1). Part of the predicted amino acid sequence of the NIPI-3 is compared to that of human Tribbles homolog 1 (TRIB1; accession number AAH63292). The N-terminal region outside the kinase domain is underlined; the site corresponding to the *nipi-3* mutation is marked by an asterisk. Identical residues are boxed in black, similar residues in grey, using Hofmann and Baron's Boxshade.

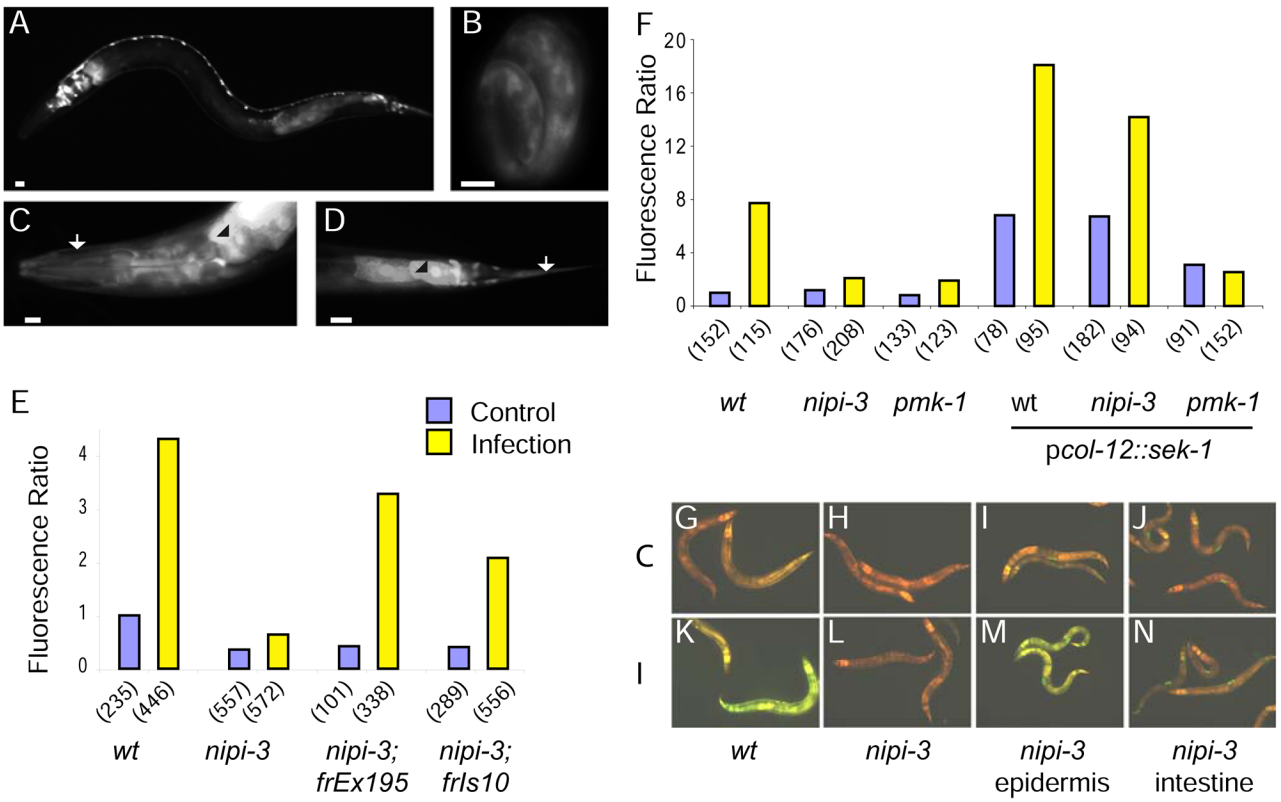

Figure 6.

A–D Fluorescence images of p*nipi-3*::GFP transgenic worms showing expression in the intestine, head neurons and motoneurons in a L1 larva (A), in the epidermis in a 3-fold embryo (B). In the adult head (C) and tail (D), expression is seen in the epidermis (arrow) and intestine (arrowhead), as well as a subset of neurons. Scale bar 10 μm. **E, F** Quantification with the Biosort of the normalized fluorescence ratio of worms carrying the *frIs7* transgene following infection (yellow) compared to controls (blue). *wt* and *nipi-3(fr4)* mutants, with or without the rescuing transgene containing *nipi-3* under its own promoter (E). *wt*, *nipi-3(fr4)* and *pmk-1* mutants, with or without the transgene containing *sek-1* under the control of the *col-12* promoter (F). **G–N** Images of uninfected (G, H, I, J) or infected (K, L, M, N) worms carrying the *frIs7* transgene in the *wt* (G, K) and *nipi-3* background (H–L), and in some cases a second transgene driving expression of *nipi-3* in the epidermis (I, M) or intestine (J, N). The worms shown in (M) are representative only of the rescued worms (see Suppl. Figure 6).

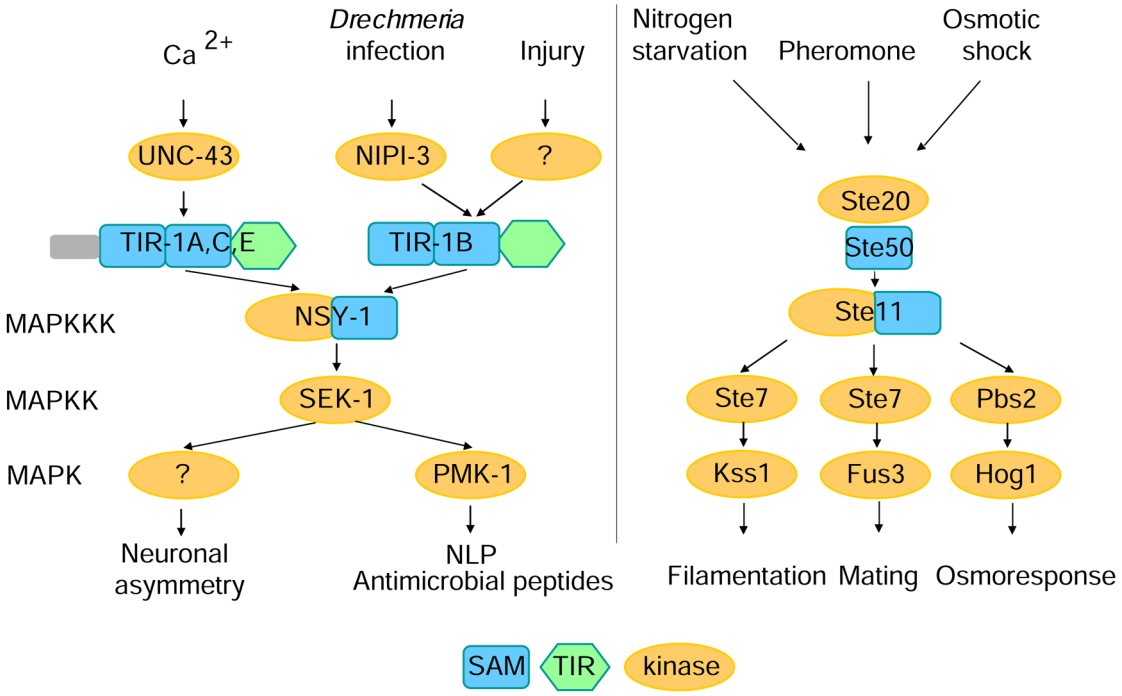

Figure 7.
Multiple signals converge on a p38 MAPK signaling cassette conserved between *C. elegans* (left panel) and budding yeast (right). NIPI-3 may function analogously to UNC-43 as an activator of TIR-1, specifically in the response to infection.